



**HAL**  
open science

## Spectral reflectance and transmittance of stacks of nonscattering films printed with halftone colors

Mathieu Hébert, Jacques Machizaud

► **To cite this version:**

Mathieu Hébert, Jacques Machizaud. Spectral reflectance and transmittance of stacks of nonscattering films printed with halftone colors. *Journal of the Optical Society of America. A Optics, Image Science, and Vision*, 2012, 29 (11), pp.2498-2508. hal-00746040

**HAL Id: hal-00746040**

**<https://hal.science/hal-00746040>**

Submitted on 26 Oct 2012

**HAL** is a multi-disciplinary open access archive for the deposit and dissemination of scientific research documents, whether they are published or not. The documents may come from teaching and research institutions in France or abroad, or from public or private research centers.

L'archive ouverte pluridisciplinaire **HAL**, est destinée au dépôt et à la diffusion de documents scientifiques de niveau recherche, publiés ou non, émanant des établissements d'enseignement et de recherche français ou étrangers, des laboratoires publics ou privés.

# Spectral reflectance and transmittance of stacks of nonscattering films printed with halftone colors

Mathieu Hébert\* and Jacques Machizaud

Université de Lyon, Université Jean-Monnet de Saint-Etienne, CNRS, UMR 5516, Laboratoire Hubert Curien, Saint-Etienne F-42000, France

\*Corresponding author: mathieu.hebert@univ-st-etienne.fr

Received June 25, 2012; revised August 20, 2012; accepted September 6, 2012;  
posted September 10, 2012 (Doc. ID 171179); published October 25, 2012

This paper combines and extends two optical models based on a two-collimated-flux approach that we previously proposed for the reflectance and transmittance of nonscattering elements, i.e., stacked nonscattering plastic films on the one hand, and films printed in halftone on the other hand. Those two models are revisited and combined by introducing different reflectances and transmittances on the two sides of a printed film, a common situation in practice. We then address the special case of stacks of identical films for which we obtain closed-form expressions for the reflectance and transmittance of the stacks as functions of the number of films. Experimental testing has been carried out on several different films printed with an inkjet printer. The accuracy of the model is good up to 16 films in most cases, despite a slight decrease in the case of yellow ink, which is more scattering than the other inks. By transposing the model to thin diffusing layers and considering diffuse fluxes instead of collimated ones, the closed-form expressions yield the well-known Kubelka–Munk reflectance and transmittance formulas. When these stacks of films are backed by a colored specular reflector, the reflectance is in certain conditions independent of the number of films. © 2012 Optical Society of America

OCIS codes: 120.5700, 120.7000, 330.1690, 100.2810.

## 1. INTRODUCTION

The visual appearance of stratified surfaces results from complex physical phenomena. This complexity makes it difficult to model, and it is scarcely possible to represent them accurately without a thorough knowledge of optics and material sciences and/or advanced skills in computational mathematics. In some special cases, however, simple formulas combined with easily measurable quantities have a good predictive performance. This is the case of strongly diffusing layers for which the description of the mutual exchange of two perfectly diffuse fluxes flowing in opposite directions, known as the Kubelka–Munk two-flux model, yields analytical formulas [1]. The amazing success of this theory in scientific and technical domains is due to the easy handling of these formulas. More than 80 years after their first publication, color reproduction specialists keep investigating its capacity to yield accurate predictions in various application domains beyond the limits drawn by its fundamental assumptions [2–6]. Piles of thick nonscattering media, even though less studied than the diffusing multilayers, are a second example of stratified media where simple formulas apply despite the infinity of possible paths followed by light before being reflected or transmitted. These formulas, presented in a previous study [7], provide a good prediction accuracy for stacks of nonscattering polymer sheets. They are also issued from a two-flux model similar to the Kubelka–Munk theory, except for the fact that the fluxes are collimated instead of being diffuse. Reflectance and transmittance of the sample are therefore angular functions, whereas those of strongly diffusing media are not. Indeed, aside from that important physical difference, the similarity between the models for nonscattering films and

the Kubelka–Munk model is an interesting issue that will be developed at the end of this paper.

In this work, we propose to explore the limitations of this model and to adapt it to cases where its assumptions are not exactly satisfied. We especially address stacks of films printed in halftone. Two assumptions of the model for stacked films are not satisfied: homogeneity of the substrates and absence of scattering. Substrate volumes are not homogeneously colored because the absorbing substances, i.e., the inks, are deposited on the surface without covering it completely. Emmel *et al.* [8] proposed a first model for the spectral transmittance of halftone printed films, based on a description of the multiple reflections of light between the film surfaces. We extend this model in order to predict both reflectance and transmittance and to take into account the fact that light may cross different ink dots during the multiple reflection process, yielding an effect similar to the Yule–Nielsen effect in paper prints [9,10]. Regarding the assumption of nonscattering, it is in opposition with the fact that most pigmented inks are slightly scattering. It is therefore an issue to verify whether accurate predictions can be achieved in practice with printed films according to the number of stacked films.

In order to provide the largest overview of what can be predicted using this two-flux angular approach, we first review light reflection and transmission by a nonscattering film (Section 2) and by films printed with halftone colors (Section 3). Section 4 is dedicated to stacks of printed films. Since the inked and noninked faces of films have slightly different reflectances, we extend the reflectance and transmittance prediction model previously proposed in [7] so as to represent the reflectances and transmittances on each side

as distinct parameters in the equations. This constitutes the first main contribution of this paper since it seems that, for the first time, the two-flux approach is used with nonsymmetric nonscattering elements. In Section 5, we deal with the special case where all stacked films are identical; we present closed-form expressions under a fractional form in which the number of films appears as a simple parameter. These expressions are the second main contribution of this paper since they had not been obtained at the time of the previous study on polymer sheets. Stacks are then placed above a specular colored background (Section 6). We analyze the variation of spectral reflectance of the specimens as the number of films increases. An interesting invariant property appears in specific conditions; its mathematical rationale is explained. In each section, experiments are presented and discussed in order to validate the models and estimate to which extent the media, especially the inks, can deviate from the assumption of nonscattering. We will see that scattering may impair the prediction accuracy when it is too strong or when the number of films increases. However, an alternative calibration permits us to reach acceptable accuracy for visual rendering purpose up to 16 stacked films, expanding the model to what appears to be the limits of the two-flux angular approach.

## 2. REFLECTANCE AND TRANSMITTANCE OF NONSCATTERING FILMS

Let us consider a nonscattering film with flat and parallel surfaces whose thickness  $h$  is much larger than the time coherence length of visible light. Interferences are thus insignificant and models based on incoherent optics laws apply. The film substrate has a real refractive index  $n_1$  and a spectral absorption coefficient  $\alpha(\lambda)$ . According to Beer's law, the attenuation of a collimated spectral flux traveling a distance  $x$  within the film substrate is  $\exp(-\alpha(\lambda)x)$ . Hence, the spectral transmittance of the film substrate for a collimated light crossing it perpendicularly, called "normal transmittance," is

$$t(\lambda) = e^{-\alpha(\lambda)h}. \tag{1}$$

If the light path forms an angle  $\psi$  with respect to the layer's normal, its path length across the film is  $h/\cos\psi$ , and its spectral angular transmittance is

$$[t(\lambda)]^{1/\cos\psi}. \tag{2}$$

At the surface of the film, light is reflected and refracted, which generates an infinite number of flux components each following a different number of internal reflections within the film. Let us denote  $\theta$  the incident angle of light coming from air and  $r_\theta$  the Fresnel angular reflectance of the surfaces at incidence  $\theta$  on air side [11]. The refraction angle of the light is given by Snell's law:

$$\theta_1 = \arcsin(\sin\theta/n_1). \tag{3}$$

For light coming from the film bulk at this angle  $\theta_1$ , the reflectance is also  $r_\theta$ . The transmittance is  $1 - r_\theta$ .

Let us describe the first flux components exiting the film. The first component is specularly reflected by the front interface; it is a fraction  $r_\theta$  of incident flux. The second one is refracted into the film, with the following attenuation factor:

$$t(\theta, \lambda) = [t(\lambda)]^{1/\cos\theta_1} = [t(\lambda)]^{n_1/\sqrt{n_1^2 - \sin^2\theta}}. \tag{4}$$

Then it is refracted again into air at the back side, representing the fraction  $(1 - r_\theta)^2 t(\theta, \lambda)$  of the incident flux. The third component is refracted into the film, attenuated a first time into the film, then reflected by the back surface and attenuated a second time across the film before being refracted again into air at the front side; it is the fraction  $(1 - r_\theta)^2 r_\theta t^2(\theta, \lambda)$  of the incident flux, and so on (see Fig. 1).

By summing up the different components exiting at each side of the film, one obtains a geometrical series that can be summed under the following closed-form formula for the spectral angular reflectance of the film:

$$R(\theta, \lambda) = r_\theta + \frac{(1 - r_\theta)^2 r_\theta t^2(\theta, \lambda)}{1 - r_\theta^2 t^2(\theta, \lambda)}, \tag{5}$$

and the following one for its spectral angular transmittance:

$$T(\theta, \lambda) = \frac{(1 - r_\theta)^2 t(\theta, \lambda)}{1 - r_\theta^2 t^2(\theta, \lambda)}. \tag{6}$$

Equations (5) and (6) are valid for either  $p$ - or  $s$ -polarization of light, using the corresponding Fresnel formulas for the surface angular reflectance. With natural incident light, the film reflectance is the average of the  $p$ -polarization and  $s$ -polarization reflectance contributions. However, we observed that with typical films used for inkjet printing, it is almost identical to use the Fresnel angular reflectance defined for natural light, i.e., to average the Fresnel coefficients before summing rather than the opposite, which provides simpler equations.

At normal incidence ( $\theta = \theta_1 = 0$ ), the angular reflectance of the surfaces is  $(n_1 - 1)^2/(n_1 + 1)^2$ . The film's transmittance expressed by Eq. (6) thus becomes

$$T(0, \lambda) = \frac{16n_1^2 t(\lambda)}{(n_1 + 1)^4 - (n_1 - 1)^4 t^2(\lambda)}. \tag{7}$$

If not known, the refractive index  $n_1$  may be assumed to be 1.5, which is a typical value for polymers. By measuring  $T(0, \lambda)$ , one deduces the normal transmittance  $t(\lambda)$  given by the following relation issued from Eq. (7):

$$t(\lambda) = \frac{\sqrt{64n_1^4 + (n_1^2 - 1)^4 T^2(0, \lambda) - 8n_1^2}}{(n_1 - 1)^4 T(0, \lambda)}. \tag{8}$$

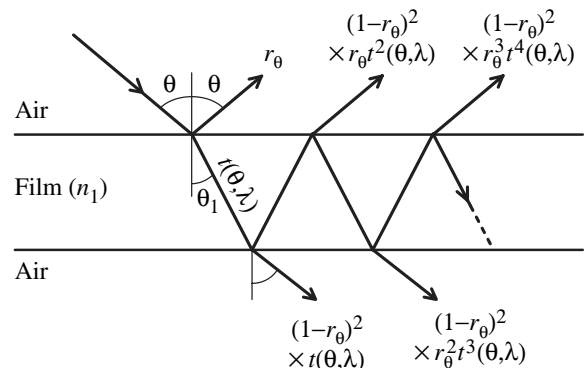


Fig. 1. Trajectories of collimated light within a transparency.

Equations (5)–(8) remain valid when the film is coated with a thick layer of nonscattering substance whose index is close to  $n_1$ . In this case, the normal transmittance given by formula (8) accounts for light absorption by both film bulk and coating.

### 3. REFLECTANCE AND TRANSMITTANCE OF PRINTED FILMS

Since the model presented above is valid when the film is coated by a nonscattering layer, it can be applied with a—not too much scattering—ink. It is also valid with halftones where the ink covers a fraction of the film surface provided the observed area is large enough to measure relevant average reflectances and transmittances. We will consider that the inked face of films is in front of the observer.

A halftone is a mosaic of colored areas resulting from the partial overlap of the ink dot screens. The areas without ink, those with a single ink layer, and those with two or three superposed ink layers are each one considered as a distinct “colorant,” also called “Neugebauer primary.” For three primary inks, e.g., cyan, magenta and yellow, one obtains a set of eight colorants: white (no ink), cyan alone, magenta alone, yellow alone, red (magenta and yellow), green (cyan and yellow), blue (cyan and magenta), and black (cyan, magenta, and yellow). In classical clustered dot halftoning or error diffusion, the fractional area  $a_k$  occupied by each colorant can be deduced from the surface coverages  $x_c$ ,  $x_m$ , and  $x_y$  of the three primary inks according to Demichel’s equations [12]

$$\begin{aligned} a_w &= (1 - x_c)(1 - x_m)(1 - x_y), \\ a_c &= x_c(1 - x_m)(1 - x_y), \\ a_m &= (1 - x_c)x_m(1 - x_y), \\ a_y &= (1 - x_c)(1 - x_m)x_y, \\ a_{m+y} &= (1 - x_c)x_mx_y, \\ a_{c+y} &= x_c(1 - x_m)x_y, \\ a_{c+m} &= x_cx_m(1 - x_y), \\ a_{c+m+y} &= x_cx_mx_y. \end{aligned} \quad (9)$$

We denote  $R_k(\theta, \lambda)$  and  $T_k(\theta, \lambda)$  the angular reflectance, respectively transmittance, of a film wholly covered by one of the eight colorants, labeled  $k$ . When the film is coated with halftone inks, we assume in a first approach as in [8] that the colorant areas contribute to the print’s angular reflectance proportionally to their respective surface coverages  $a_k$

$$R(\theta, \lambda) = \sum_{k=1}^8 a_k R_k(\theta, \lambda). \quad (10)$$

This model, known as the spectral Neugebauer model, may be noticeably improved by applying to Eq. (10) the Yule–Nielsen transform as suggested by Viggiano [13]

$$R(\theta, \lambda) = \left[ \sum_{k=1}^8 a_k R_k^{1/n}(\theta, \lambda) \right]^n, \quad (11)$$

where  $n$  is a number to be fitted in the calibration step. The Yule–Nielsen transform, well known for paper prints [9,10], empirically models the nonlinear relationship between halftone reflectance and individual colorant reflectances

due to the complex paths of scattered light in the paper that cross several colorant areas [14]. In the case of printed films, scattering is much less pronounced. However, at oblique incidence, light also shifts from colorant areas to other ones during the multiple reflection process.

The extension of the Yule–Nielsen reflectance model to transmittance, experimentally validated in the case of printed papers [15], remains valid for printed films. The transmittance equation is similar to the reflectance equation (11), with an  $n$ -value that is generally different in transmittance mode versus reflectance mode:

$$T(\theta, \lambda) = \left[ \sum_{k=1}^8 a_k T_k^{1/n}(\theta, \lambda) \right]^n. \quad (12)$$

Calibration of the reflectance and transmittance models follows the procedure detailed in [15]. Using spectral measurements, one has to determine the reflectances and transmittances of the colorants as well as the amount of spreading of the ink dots in halftones. Let us recall this procedure in the specific case of printed films.

In a first step, each of the eight colorants  $k = 1, \dots, 8$  is printed separately on the film. Its spectral reflectance  $R_k(0, \lambda)$  and spectral transmittance  $T_k(0, \lambda)$  are measured at normal incidence. These measurements are sufficient for the prediction of halftone reflectances or transmittances at normal incidence using Eq. (11), respectively Eq. (12). If one rather wants to make predictions at oblique incidence, unless the eight angular reflectances and the eight angular transmittances can be measured at this angle, one has to compute them. For this purpose, one uses the eight measured transmittances  $T_k(0, \lambda)$  to compute the eight normal transmittances  $t_k(\lambda)$  using Eq. (8), then the eight angular transmittances  $t_k(\theta, \lambda)$  using Eq. (4) for the considered incident angle  $\theta$ , and finally the eight colorant angular reflectances  $R_k(\theta, \lambda)$  and transmittances  $T_k(\theta, \lambda)$  using Eq. (5), respectively Eq. (6).

In a second step, the spreading of the ink dots is assessed knowing that spreading depends on the nominal surface coverage of the dots and on their eventual superposition with other inks [16]. Spectral measurements are performed on specific halftones where the nominal surface coverage of one ink is  $a = 0.25, 0.5, \text{ or } 0.75$ , and the nominal surface coverage of each of the two other inks is 0 or 1. This forms a set of 36 halftones, each one containing two colorants: the colorant out of the halftone dots labeled  $u$ , which covers a fractional area  $1 - a$ , and the colorant in the dots, obtained by superposition of ink  $i$  and colorant  $u$ , labeled  $i + u$ , which covers a fractional area  $a$ . According to Eq. (12), the spectral reflectance at normal incidence of each of these 36 halftones is given by

$$R_{i/u}(a, \lambda) = [(1 - a)R_u^{1/n}(0, \lambda) + aR_{i+u}^{1/n}(0, \lambda)]^n. \quad (13)$$

Surface coverage  $a$  is fitted in order to optimize the agreement between the predicted spectral reflectance,  $R_{i/u}(a, \lambda)$ , and the measured one,  $R_m(\lambda)$ . The optimal  $a$  value, called “effective surface coverage,” minimizes the sum of squared differences between the two spectra:

$$a_{i/u} = \arg \min_a \left[ \sum_{\lambda} (R_{i/u}(a, \lambda) - R_m(\lambda))^2 \right]. \quad (14)$$

Repeating this process for the 36 halftones, one gets the effective surface coverages associated with the nominal surface coverages 0.25, 0.5, and 0.5 for each ink—colorant pair  $i/u$ . In order to determine the optimal  $n$  value, one can test various values and select the one for which the average metric computed in Eq. (14), i.e., the sum of square differences between predicted and measured spectral reflectances, is minimal. One assumes that nominal surface coverage 0 (no ink) and 1 (full coverage) yields effective surface coverage 0, respectively 1. By linear interpolation between these points, one obtains 12 ink spreading functions  $f_{i/u}(a)$  giving the effective surface coverage of each ink as a function of the nominal one (a) when the ink is alone on paper, or (b) when it is superposed with a second ink, (c) superposed with the third ink, or (d) superposed with the two other inks (see [15,16]).

Let us now show how to predict the reflectance and transmittance of a three-ink halftone defined by the nominal surface coverages  $c$ ,  $m$ , and  $y$  for the cyan, magenta, and yellow inks, respectively. The corresponding effective surface coverages are obtained by a weighted average of the ink spreading functions  $f_{i/u}$ . The weights are expressed by the surface coverages of the colorants  $u$  in the halftone. For example, the weight of the ink spreading function  $f_{c/w}$  (cyan halftone over white colorant) is  $(1 - x_m)(1 - x_y)$ , where  $x_m$  and  $x_y$  denote the effective surface coverage of the magenta, respectively yellow, inks. The effective surface coverages are obtained by performing a few iterations with the following equations:

$$\begin{aligned} x_c &= (1 - x_m)(1 - x_y)f_{c/w}(c) + x_m(1 - x_y)f_{c/m}(c) + (1 - x_m)x_yf_{c/y}(c) + x_mx_yf_{c/m+y}(c), \\ x_m &= (1 - x_c)(1 - x_y)f_{m/w}(m) + x_c(1 - x_y)f_{m/c}(m) + (1 - x_c)x_yf_{m/y}(m) + x_cx_yf_{m/c+y}(m), \\ x_y &= (1 - x_c)(1 - x_m)f_{y/w}(y) + x_c(1 - x_m)f_{y/c}(y) + (1 - x_c)x_mf_{y/m}(y) + x_cx_mf_{y/c+m}(y). \end{aligned} \quad (15)$$

For the first iteration,  $x_c = c$ ,  $x_m = m$ , and  $x_y = y$  are taken as initial values on the right-hand side of the equations. The obtained values of  $x_c$ ,  $x_m$ , and  $x_y$  are then inserted again into the right side of the equations, which gives new values of  $x_c$ ,  $x_m$ , and  $x_y$  and so on, until the values of  $x_c$ ,  $x_m$ ,  $x_y$  stabilize. The effective surface coverages of the colorants,  $a_k$ , are calculated by plugging the obtained values for  $x_c$ ,  $x_m$ , and  $x_y$  into the Demichel equations (9). Finally, with the colorant reflectances  $R_k(\theta, \lambda)$  and transmittances  $T_k(\theta, \lambda)$  and the colorant surface coverages  $a_k$  provided by the Demichel equations, Eqs. (11) and (12) yield the spectral reflectance, respectively transmittance, of the film printed with the considered halftone color.

We tested the reflectance and transmittance prediction model for halftones printed in inkjet on 3 M CG3460 transparency films. One hundred twenty-five halftones were printed, corresponding to combinations of cyan, magenta, and yellow inks printed each one at a nominal surface coverage of 0, 0.25, 0.5, 0.75, or 1. Each one is measured in reflectance and transmittance modes at normal incidence ( $\theta = 0$ ) with the X-rite Color i7 spectrophotometer. This instrument provides diffuse illumination thanks to an integrating sphere; samples are placed against the sphere. However, in the case of a nonscattering sample, only the luminance normal to the sample goes

**Table 1. Prediction Accuracy of the Model for Spectral Reflectance and Transmittance of Printed Films**

Measurement Mode	Optimal $n$ value	Average $\Delta E_{04}$	95%-Quantile
Reflectance	10	0.15	0.48
Transmittance	2	0.34	0.87

to the detector; the geometry is therefore a  $0^\circ:0^\circ$  geometry; see [17]. Reflectance predictions are based on Eq. (11) and transmittance predictions on Eq. (12). In order to assess the deviation between predicted and measured spectra in respect to the human vision, we use the CIELAB  $\Delta E_{94}$  color distance obtained by converting the predicted and measured spectra into CIE-XYZ tristimulus values, calculated with a D65 illuminant and in respect to the  $2^\circ$  standard observer, then by converting the CIE-XYZ values into CIELAB color coordinates using as white reference the spectral reflectance of a perfect diffuser illuminated with the D65 illuminant [18]. The average color distance for each mode, presented in Table 1, is less than 0.4, therefore lower than the perceptible color difference threshold, which is generally assumed to be 1. The achieved prediction accuracy is therefore satisfying.

In theory, printed films should have the same reflectance and transmittance on their two faces. Flipping them without changing the illumination and observation conditions should

not modify their visual aspect. However, optical phenomena such as scattering or the bronzing effect may generate a colored sheen visible in reflectance only on the face with ink. It is therefore important to pay attention to the observed face. The model calibrated from measurements on one face is specific to this face. The prediction of the spectral reflectance or transmittance on the other face needs a second model, similar to the first one but calibrated from measurements on this face.

We can illustrate such difference with the Canon inkjet cyan ink used in our experiments: on the inked face in the specular direction, areas where cyan ink is not covered by other inks display a purplish aspect that is not observed on the other face. The spectral reflectances on the inked face (“front side”) and noninked face (“back side”) of a film printed with cyan ink at full surface coverage are plotted in Fig. 2. The higher reflectance measured on the inked face below 350 nm and beyond 550 nm is at the origin of the purplish sheen, while the opposite face has a bluish color characteristic of cyan ink deposited on a weakly reflecting support. In transmittance, the difference between front and back sides is much smaller. We can consider with inkjet prints that the relative difference between the two transmittances, generally inferior to 1%, is independent of wavelength.

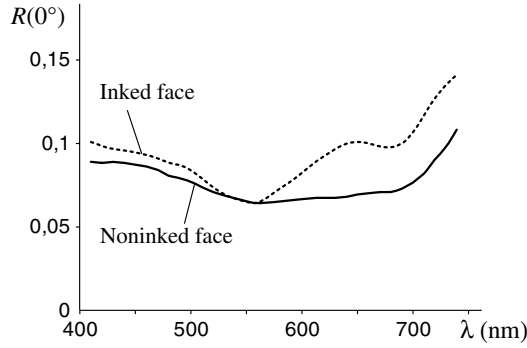


Fig. 2. Spectral reflectance measured at normal incidence on the inked face (dotted curve) and the opposite face (solid curve) of a film printed with cyan and yellow inks at surface coverages 0.57, respectively 0.12.

### 4. STACKS OF PRINTED FILMS

In this section, we consider stacks of several printed films parallel to each other. The corresponding spectral reflectance and transmittance model is similar to the one introduced in [7] for stacks of nonscattering plastic sheets, except that here we consider a more general case where the films have different spectral reflectances and transmittances when illuminated at the front and back sides. The model describes the multiple reflections of collimated light between the films, assuming that even though the films are in contact with each other in a mechanical point of view, they are not in optical contact unless a fluid is used to paste them to each other: there remains a layer of air between them in which light has a same orientation as the incident light (angle  $\theta$ ), or a symmetric orientation with respect to the normal of the films (“regular” or “specular” direction, with same angle  $\theta$ ). The angular reflectances and transmittances of stacks are functions of the individual angular reflectances and transmittances of films all evaluated at this angle  $\theta$ . In order to simplify the notations, we will omit dependence on angle  $\theta$  and on wavelength  $\lambda$  in the general equations.

Let us first consider two films labeled with numbers 1 and 2, label 1 being attached to the film located at the back side. Their front and back reflectances and front-to-back and back-to-front transmittances are respectively denoted as  $R_i$ ,  $R'_i$ ,  $T_i$ , and  $T'_i$  ( $i = 1, 2$ ). Figure 3 represents the multiple reflections between the two films as well as the first fractions of flux exiting at the front and back sides.

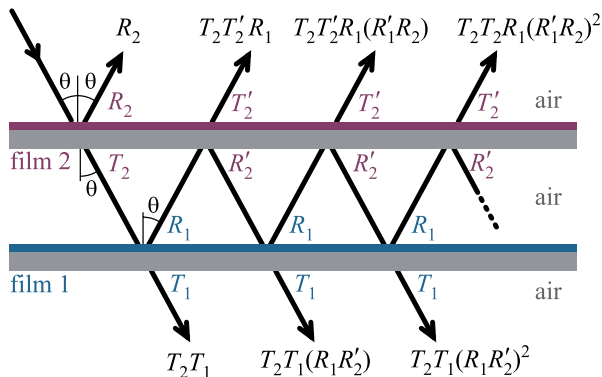


Fig. 3. (Color online) Multiple reflections of collimated flux between two nonscattering films.

By summing up the fractions of flux exiting at the front side, one obtains a geometrical series expressing the front reflectance of the two-stack, which reduces as

$$R_{21} = R_2 + \frac{T_2 T'_2 R_1}{1 - R_1 R'_2} \tag{16}$$

At the back side, the summation of fractions of flux also constitutes a geometrical series, which expresses the front-to-back transmittance:

$$T_{21} = \frac{T_2 T_1}{1 - R_1 R'_2} \tag{17}$$

A similar reasoning for incident light coming from the back side at the same angle gives the following expression for the back reflectance:

$$R'_{21} = R'_1 + \frac{T_1 T'_1 R'_2}{1 - R_1 R'_2} \tag{18}$$

and the back-to-front transmittance:

$$T'_{21} = \frac{T'_1 T'_2}{1 - R_1 R'_2} \tag{19}$$

Expressions like (16)–(18) can be given when a film  $q$  is in front of a stack of  $p$  films. The reflectances and transmittances of the  $p$  films (subscript  $p \dots 1$ ) are related to those of the  $q$  films (subscript  $qp \dots 1$ ) as

$$R_{qp \dots 1} = R_q + \frac{T_q T'_q R_{p \dots 1}}{1 - R_{p \dots 1} R'_q} \tag{20}$$

$$T_{qp \dots 1} = \frac{T_q T_{p \dots 1}}{1 - R_{p \dots 1} R'_q} \tag{21}$$

$$R'_{qp \dots 1} = R'_{p \dots 1} + \frac{T'_{p \dots 1} T'_{p \dots 1} R'_q}{1 - R_{p \dots 1} R'_q} \tag{22}$$

$$T'_{qp \dots 1} = \frac{T'_q T'_{p \dots 1}}{1 - R_{p \dots 1} R'_q} \tag{23}$$

Equations (20)–(23) are similar to Kubelka’s equations for stacked diffusing layers because they are consequences of a similar mathematical model [19]. However, they have different physical meaning: Kubelka’s equations model the propagation of *diffuse* light in *diffusing* stratified media and therefore rely on *diffuse* reflectances and transmittances whereas the above equations model the propagation of *collimated* light in *nonscattering* stratified media and rely on *angular* reflectances and transmittances. Nevertheless, this mathematical analogy is interesting, in particular when the films are identical since specific formulas presented in the next section are connected to the Kubelka–Munk model (see Section 8).

In order to obtain the reflectances and transmittances of a given stack of films whose individual reflectances and transmittances are known, one may iteratively use Eqs. (20)–(22). In the first iteration, films 1 and 2 are considered, and then one obtains the reflectances and transmittances of this two-stack;

**Table 2. Prediction Accuracy for the Spectral Transmittance of Stacks of Printed Films**

Number of Stacked Films	Average $\Delta E_{94}$	95%-Quantile
2	0.55	2.03
3	0.69	1.36
4	0.86	1.36

in a second step, one considers film 3 in front of the previous two-stack and so on, until film  $N$  is considered in front of the previous  $(N - 1)$ -stack.

By experimental testing, we predicted the spectral transmittances of stacks of two, three, and four printed films. On each film, 25 randomly selected halftones were printed in the same positions; in this way, every film superposition has given 25 colored samples. The same films and printer were used as for the experiment presented in Section 3 and the halftones were generated by the stochastic screening algorithm proposed in [20] in order to prevent moirés. Measurements were performed at normal incidence. Using the model presented in Section 3, duly calibrated from the spectral reflectance and transmittance measurement of the 44 specific halftones, we predicted the spectral reflectance and transmittance of all halftones (25 per film), assuming that both film faces have same reflectance. We then predicted the spectral transmittances of the samples and compared them to measurements in terms of equivalent color distance by CIELAB  $\Delta E_{94}$  values. The average  $\Delta E_{94}$  values presented in Table 2 (over 25 samples), all below 0.9, are comparable to the ones typically obtained for halftones printed on paper in transmittance mode [15]. Despite the error accumulation due to the  $2N + 1$  predictions performed for  $N$  stacked films (reflectance and transmittance of each film, then transmittance of the stack), we can consider that a good accuracy has been achieved in this experiment.

## 5. STACKS OF IDENTICAL FILMS

Let us now focus on the special case where  $N$  identical films are stacked together. The stack's front and back reflectances and front-to-back and back-to-front transmittances are respectively denoted as  $R_N, R'_N, T_N,$  and  $T'_N,$  and those of individual films are denoted as  $R, R', T,$  and  $T'.$  As shown in Appendix A, the iterative use of Eqs. (20)–(22) yields in this case closed-form formulas for  $R_N, R'_N, T_N,$  and  $T'_N.$  The formula for the front reflectance is

$$R_N = \frac{1}{\alpha - \beta \left( 1 - \frac{2}{1 - \left[ \frac{1 - (\alpha + \beta)R}{1 - (\alpha - \beta)R} \right]^N} \right)}, \quad (24)$$

and the formula for the front-to-back transmittance is

$$T_N = \frac{2bT^N}{(\alpha + \beta)[1 - (\alpha - \beta)R]^N - (\alpha - \beta)[1 - (\alpha + \beta)R]^N}, \quad (25)$$

where  $\alpha$  and  $\beta$  are functions of  $R, R', T,$  and  $T';$  therefore of angle and wavelength are defined as

$$\alpha = \frac{1 + RR' - TT'}{2R}, \quad (26)$$

and

$$\beta = \sqrt{\alpha^2 - \frac{R'}{R}}. \quad (27)$$

The front and back reflectances are related according to

$$R'_N = R_N \frac{R'}{R}, \quad (28)$$

and the front-to-back and back-to-front transmittance according to

$$T'_N = T_N \left( \frac{T'}{T} \right)^N. \quad (29)$$

As  $N$  tends to infinity, the transmittance  $T_N$  tends to zero and the front reflectance asymptotically converges toward a spectral angular reflectance called “infinite stack reflectance,” denoted as  $R_\infty.$  Since an infinite stack is unchanged when one film is added on it, we can write Eq. (20):

$$R_\infty = R + \frac{TT'R_\infty}{1 - R_\infty R'}. \quad (30)$$

Solving Eq. (30) for  $R_\infty,$

$$R_\infty = (\alpha - \beta) \frac{R}{R'} = \frac{1}{\alpha + \beta}. \quad (31)$$

According to Eq. (28), the reflectance of an infinite stack of films observed from the back side is given by

$$R'_\infty = \alpha - \beta = \frac{R'}{R} \cdot \frac{1}{\alpha + \beta}. \quad (32)$$

By way of example, we plotted in Fig. 4 the spectral front reflectance and the front-to-back spectral transmittance of 1–16 films printed in inkjet with a halftone of green ink at 50% surface coverage, measured at normal incidence. As  $N$  gets larger, the reflectance increases and asymptotically converges toward the infinite stack reflectance plotted as a dashed line, which has been obtained from formula (31). This increase is due to the back-reflection of light at the interfaces. It is naturally less pronounced in the spectral domains where the ink is more absorbing. Regarding the transmittance, since transmission through a film is lowered by both absorption and back-reflection, transmittance decreases as  $N$  increases and asymptotically tends to zero. These variations as a function of  $N$  are perfectly similar to those extensively detailed in [7] in the case of colored nonscattering plastic sheets.

Using Eq. (23), one may deduce  $T$  from the measurement of  $R_{k-1}, T_{k-1},$  and  $T'_k$  for a given  $k:$

$$T = \frac{T'_k}{T_{k-1}} (1 - R_{k-1}R'). \quad (33)$$

In the case where scattering of light by the inks is observed, the scattering effect is more sensible in a stack of  $k$  films than in a single film. The  $T$  spectrum deduced from Eq. (33) may therefore provide better predictions than the one measured directly on one film.

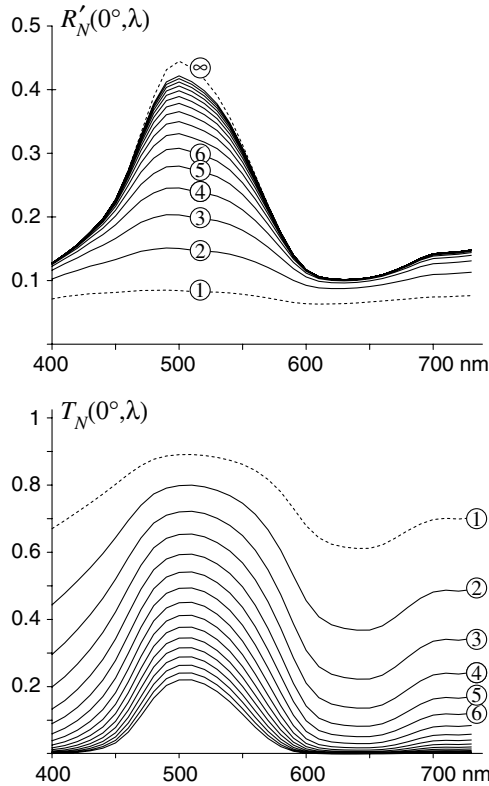


Fig. 4. Spectral front reflectances (top graph) and front-to-back transmittances (bottom graph) of single green film (dashed curves) and of stacks of 2–16 green films (solid curves) measured at normal incidence. The numbers of films in the stack appear as circled. Infinite stack reflectance denoted by symbol  $\infty$  is predicted according to formula (31).

We tested the model using as previously 3M CG3460 films printed in inkjet. In order to study the influence of the inks on the prediction accuracy, we selected four colors generated by error diffusion halftoning, which will be called “green,” “blue,” “magenta,” and “yellow” samples. They were produced by

**Table 3. Average (max)  $\Delta E_{94}$  Values Obtained for the Different Films and Geometries**

Film Color	$\gamma$ value	$R_N$	$R'_N$	$T_N$
Green	0.994	0.12 (0.23)	0.45 (0.64)	0.49 (0.96)
Blue	0.993	0.24 (0.30)	0.50 (0.63)	0.35 (0.74)
Magenta	0.993	0.39 (0.43)	0.20 (0.24)	1.21 (1.68)
Yellow	0.990	0.55 (0.68)	0.97 (1.17)	2.41 (3.94)

printing cyan, magenta, yellow, and green inks at the respective surfaces coverages  $\{c, m, y, g\} = \{0, 0, 0, 0.5\}$  for green,  $\{0.35, 0.15, 0, 0\}$  for blue,  $\{0, 0.70, 0, 0\}$  for magenta, and  $\{0.10, 0.10, 0.80, 0\}$  for yellow. For each color, we measured  $R, R',$  and  $T$  on one film, then incremented the number of films and measured  $R_N, R'_N,$  and  $T_N$  until 16 films (15 film stacks are therefore measured for each of the three geometries). In this experiment, we assumed  $T' = \gamma T$ , where  $\gamma$  is a constant independent of wavelength, specified in Table 3 for each type of film. Lower  $\gamma$  coincides with higher scattering: the yellow ink is more scattering than the other inks.

Using the same protocol as in previous experiments, predicted and measured spectra are compared in terms of equivalent color distance expressed by CIELAB  $\Delta E_{94}$  values. For each film color, we predicted front reflectances, back reflectances, and front-to-back transmittances of the 15 stacks. We tested the alternative calibration based on Eq. (33) for magenta and yellow films with  $k = 4$ , respectively  $k = 5$ . For each series of 15 measurements-predictions, the evolutions of the  $\Delta E_{94}$  as a function of  $N$  for the different colors and geometries are plotted in Fig. 5, and the average (and maximal in bracket)  $\Delta E_{94}$  values are given in Table 3. First of all, we see in Fig. 5 that the front reflectances of all films are well predicted since the  $\Delta E_{94}$  values are below 1. The back reflectances are correctly predicted as well, except for the yellow films beyond eight films. However, for this later case, calibration of the transmittance  $T$  from Eq. (33) with  $k = 5$  improves noticeably the predictions: the average (respectively maximal)  $\Delta E_{94}$  value become 0.78 (respectively 0.96) instead of 0.97 (respectively 1.17). In transmittance, predictions are good for the green and blue films, but not for the magenta and yellow films beyond five films. In the case of the yellow films, the error seems to grow proportionally to the number of films. Nevertheless, the improvement due to the calibration of  $T$  from Eq. (33) is appreciable: for the magenta films, with  $k = 4$ , we get an average  $\Delta E_{94}$  value of 0.45 and a maximum of 0.90 instead of 1.21, respectively 1.68; for the yellow films, with  $k = 5$ , we get an average  $\Delta E_{94}$  value of 0.74 and a maximum of 1.25 instead of 2.41, respectively 3.94.

It is not surprising to observe a lower prediction accuracy for yellow films since the yellow ink is the more scattering. This can be easily verified by looking at far objects through different films: blurring is more pronounced with films where yellow ink is in high quantity. We can imagine more scattering inks, such as color toner in electrophotography printing for example, for which the model may be in failure even with these corrections. Empirical improvements may be found for specific cases by introducing fittable parameters;

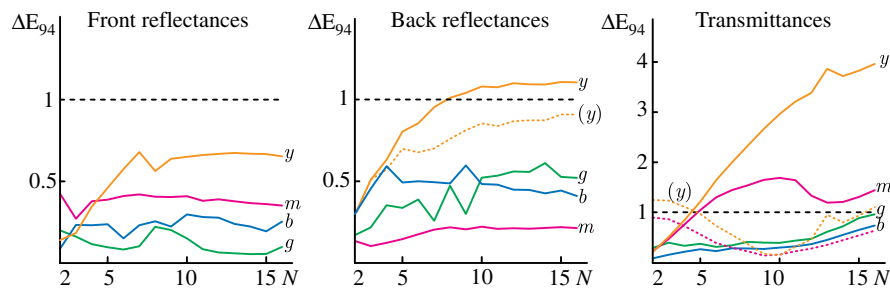


Fig. 5. (Color online) Variation of the  $\Delta E_{94}$  value as a function of the number of films for the front reflectance, the back reflectance, and the front-to-back transmittance of green (g), blue (b), magenta (m), and yellow (y) films when the single film transmittance  $T$  is measured (solid curves) or deduced from Eq. (33) (dotted curves). Horizontal dashed lines indicate the visibility threshold of color differences ( $\Delta E_{94} = 1$ ).

nevertheless, a physical scattering model based on a multiflux approach [21,22] or on the radiative transfer theory [23,24] would be more satisfying.

## 6. STACKS OF FILMS IN FRONT OF A SPECULAR REFLECTOR

We go one step further by placing the stacks of films in front of a specular reflector. Samples are still observed in the specular direction. In the general case, the reflectance of a stack with front reflectance  $R_{p...1}$ , back reflectance  $R'_{p...1}$ , front-to-back transmittance  $T_{p...1}$ , and back-to-front transmittance  $T'_{p...1}$  in front of a specular backing with reflectance  $P_0$  is given by

$$P_{p...1} = R_{p...1} + \frac{T_{p...1}T'_{p...1}P_0}{1 - P_0R'_{p...1}}. \quad (34)$$

We are especially interested in the case where the films are identical, i.e.,  $R_{p...1} = R_N$ ,  $R'_{p...1} = R'_N$ ,  $T_{p...1} = T_N$ , and  $T'_{p...1} = T'_N$ , given respectively by Eqs. (24), (28), and (25). We denote by  $P_N$  the reflectance of  $N$  films with backing. When placing an additional film, the reflectance becomes, for  $N \geq 0$ ,

$$P_{N+1} = R + \frac{TT'P_N}{1 - P_NR'}. \quad (35)$$

The variation of  $P_N$  as a function of  $N$  is shown in Fig. 6 for the blue and green films presented in Section 5 respectively placed in front of a red reflector (copper mirror covered by a film coated with red ink) and a magenta reflector (achromatic mirror covered by a film coated with magenta ink). In both cases, the number of films was incremented from 1 to 13. For the sake of readability, only the measured spectra are plotted in the figure. Using previously computed reflectances and transmittances of stacks (see Table 3), the predictions given by Eq. (35) satisfyingly match the measurements: the average  $\Delta E94$  value assessing the deviations between predicted and measured spectra was 0.42 (maximum 0.66) for the green films on magenta background, and 0.64 (maximum 0.75) for the blue films on red background.

Through these examples, one observes that as the number of films in front of the backing increases, the spectral reflectance of the samples varies differently according to the wavelength, or more precisely according to the relative values of the backing reflectance and the infinite stack reflectance. Hence,  $P_N$  either increases or decreases and may even be constant for wavelengths where the spectral reflectances of backing and infinite stack meet.

The intersection of all  $P_N(\lambda)$  at a given (set of) wavelength (s) has a theoretical justification that may be shown through the study of the variation of sequence  $P_N$  as a function of  $N$ . After some calculation using terms  $a$  and  $b$  defined by Eqs. (26) and (27), one obtains

$$P_{N+1} - P_N = \frac{R'}{1 - P_N R'} \left[ P_N - \frac{R}{R'} (\alpha - \beta) \right] \cdot \left[ P_N - \frac{R}{R'} (\alpha + \beta) \right]. \quad (36)$$

According to Eqs. (31) and (32), Eq. (36) is also written

$$P_{N+1} - P_N = \frac{R'}{1 - P_N R'} (P_N - R_\infty)(P_N - 1/R'_\infty). \quad (37)$$

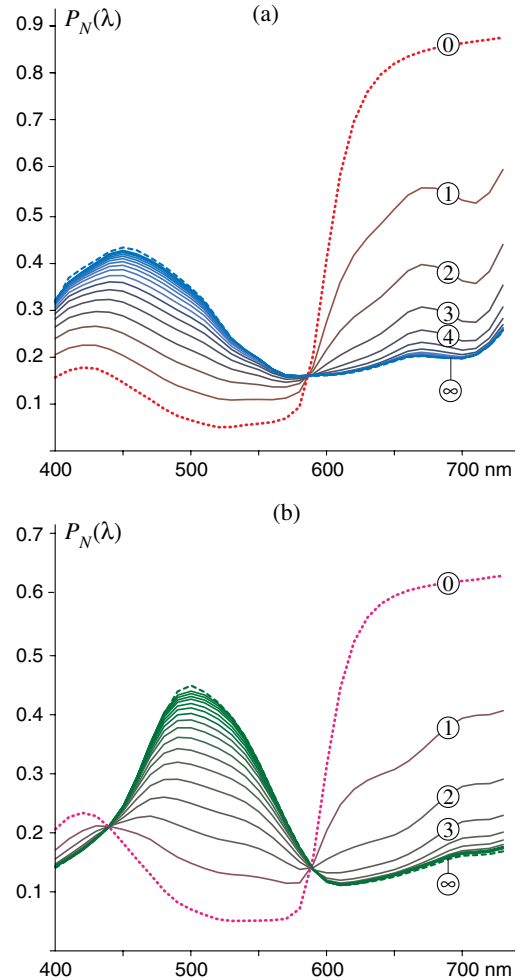


Fig. 6. (Color online) Evolution of the spectral reflectance of (a) blue films in front of a red reflector and (b) green films in front of a magenta reflector. The circled numbers denote numbers of films and line colors roughly reproduce the colors associated to the plotted spectra. Spectral reflectances of the backing alone and of an infinite stack of films are in dotted and dashed curves, respectively.

The fraction in Eq. (37) is positive. Reflectances  $P_N$  and  $R'_\infty$  being less than 1, the term  $P_N - 1/R'_\infty$  is negative.  $P_{N+1} - P_N$  has therefore an opposite sign to  $P_N - R_\infty$ . Hence, if  $P_N \leq R_\infty$  in a given spectral domain, then  $S_N \leq S_{N+1}$  and we have

$$R + \frac{TT'}{\frac{1}{P_N} - R'} \leq R + \frac{TT'}{\frac{1}{R_\infty} - R'};$$

therefore, according to Eqs. (30) and (35),  $P_{N+1} \leq R_\infty$ . We conclude that sequence  $P_N$  is increasing. Stacks without backing are a special case of this configuration with  $P_0 = 0$  for all wavelengths: we retrieve in Fig. 4 the fact that the reflectance of stacks of green films increases as  $N$  increases.

By a similar reasoning line,  $P_N$  decreases if  $P_N \geq R_\infty$ . We finally see that the reflectance of the stack with backing varies in a monotonic manner as the number  $N$  of films increases (but not necessarily in the same direction in each waveband) from the backing reflectance  $P_0$  when  $N = 0$ , to the infinite stack reflectance  $R_\infty$  when  $N \rightarrow \infty$ . If both backing and infinite stack of films have same reflectance at a given angle  $\theta$  and in a

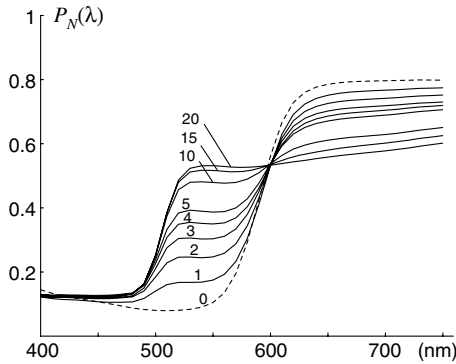


Fig. 7. Variation of the spectral reflectance of a red paper background covered by yellow films; the numbers attached to the spectra indicate the number of added films.

given waveband around wavelength  $\lambda$ , i.e., if  $R_\infty(\theta, \lambda) = P_0(\theta, \lambda)$ , then  $P_N(\theta, \lambda)$  is equal to  $P_0(\theta, \lambda)$  for every  $N$ .

In [7], we observed a similar intersection phenomenon with nonscattering colored plastic films placed in front of a diffusing background. In this case, perfect intersection of the spectral reflectances is more difficult to prove mathematically because the reflectance equations contain integrals (the angular reflectance and transmittance of the stacks are integrated over the hemisphere because the light exiting the diffusing background is Lambertian). Nevertheless, good intersection was experimentally observed. A much similar observation can be done with yellow printed films in front of a red paper background whose spectral reflectances are plotted in Fig. 7: all spectra meet in a same point, except the one of the red paper (dashed line in the figure), which is slightly higher because of the small amount of light scattered by its rough surface that is added to the light reflected from the red paper bulk. This fraction of light is not captured when films are added since they have a smooth surface.

## 7. CONNECTION WITH THE KUBELKA–MUNK MODEL

We have mentioned in Section 5 the analogy between the model for stacks of nonscattering films and Kubelka's model for stacks of diffusing layers, even though collimated light is considered in the first one and diffuse light in the second one. This analogy may be pursued between stacks of identical films and stacks of identical diffusing layers, i.e., uniform diffusing layer with varying thickness: there exists indeed a mathematical connection between the formulas introduced in Section 6 and the Kubelka–Munk formulas.

The Kubelka–Munk theory models the propagation of diffuse flux in a homogenous diffusing layer (thickness  $h$ ) by describing the flux attenuations through infinitesimal sublayers due to scattering and absorption. According to this model, denoting  $dz$  the thickness of the sublayer, a fraction  $Sdz$  of flux is back-reflected by it and a fraction  $Kdz$  is absorbed. The sublayer's reflectance is therefore  $Sdz$  (similar at front and back sides) and its transmittance is  $1 - (K + S)dz$ . In order to put into evidence the analogy with our model for stacks, we propose to divide the layer into  $N$  sublayers of equal thickness  $h/N$  in a similar manner as in [25], where a matrix approach was used. As  $N$  tends to infinity, sublayers have infinitesimal thickness and their reflectance may be written

$R = R' = Sh/N$ , and their transmittance  $T = T' = 1 - (K + S)h/N$ . Inserting these expressions for  $R$  and  $T$  into Eq. (26), we retrieve a usual expression for  $a$  in the Kubelka–Munk theory:

$$\alpha = \lim_{N \rightarrow \infty} \frac{1 + (Sh/N)^2 - [1 - (K + S)h/N]^2}{2Sh/N} = \frac{K + S}{S} = a.$$

Since  $R = R'$ ,  $\beta$  is

$$\beta = \sqrt{\alpha^2 - 1} = b.$$

The equality in this case between the parameters  $a$  and  $b$  of the Kubelka–Munk model and the parameters  $\alpha$ , respectively  $\beta$ , of our model explains why both models similarly express the reflectance of an infinitely thick sample [1]:  $R_\infty = a - b = 1/(a + b)$ .

For finite thickness, we make  $N$  tend to infinity in order to have an infinitesimal sublayer and insert  $R$ ,  $R'$ ,  $T$ ,  $T'$ ,  $a$ , and  $b$  as defined above into Eq. (24). Using a classical result for the exponential function [27],

$$\lim_{N \rightarrow \infty} \left(1 - \frac{x}{N}\right)^N = e^{-x}, \quad (38)$$

we easily retrieve the well-known Kubelka–Munk reflectance expression [1]:

$$\begin{aligned} R_{\text{km}}(h) &= \lim_{N \rightarrow \infty} R_N = \frac{1}{a - b \left(1 - \frac{2}{1 - e^{-2bSh}}\right)} \\ &= \frac{\sinh(bSh)}{a \sinh(bSh) + b \cosh(bSh)}. \end{aligned} \quad (39)$$

By a similar reasoning for the transmittance, taking into account  $T = 1 - aSh/N$ , we retrieve from Eq. (25) the Kubelka–Munk transmittance formula:

$$\begin{aligned} T_{\text{km}}(h) &= \lim_{n \rightarrow \infty} T_N = \frac{2be^{-aSh}}{(a + b)e^{-(a-b)Sh} - (a - b)e^{-(a+b)Sh}} \\ &= \frac{2b}{a \sinh(bSh) + b \cosh(bSh)}. \end{aligned} \quad (40)$$

If the diffusing layer is on top of a background, the resulting reflectance is still given by Eq. (34), where  $S_0$  is the reflectance of the background.

The similarity between the two models implies that  $K$  and  $S$  coefficients could be attributed to nonscattering films (for a given incidence angle  $\theta$ ), the  $S$  coefficient representing in this case back-reflection instead of scattering. This approach has first of all a pedagogical interest, since the reflection and absorption of light by individual film is easily seen or measured, and the influence of thickness can be easily observed by superposing films. Moreover, since back-reflection occurs at the surface of the films and absorption occurs inside, both phenomena are distinguishable. If the films are water-resistant (which is not the case of films printed in ink-jet but is true for colored polymer sheets or UV-dried offset prints), fluids with various refractive indices may be used to modify the surface reflectance of films, thereby  $S$ , without changing  $K$ . Water (index 1.33) and oil (index 1.5) were used in the study of [7] for that purpose. Conversely, the use of films made of

the same medium with different colors enables the variation of  $K$  without the need to change  $S$ . Changing  $K$  only or  $S$  only in the case of scattering media is more difficult since it generally means introducing a substance that is generally absorbing and scattering at the same time. Stacks of films therefore appear to be a good learning support to study experimentally the variation of reflectance and transmittance according to the  $K$  and  $S$  values and the thickness.

## 8. CONCLUSION

We have demonstrated the possibility to accurately predict the spectral reflectance and transmittance of stacks of films printed in halftone, provided the halftones are generated by the stochastic or error diffusion algorithm in order to avoid moirés and the inks are not too much scattering. Since the printed films have slightly different reflectances and transmittances on their two sides, these latter are represented by distinct parameters in the equations. This is original compared to most previous applications of the two-flux model. When all the stacked films are identical, their reflectance and transmittance are given by closed-form formulas that have never been presented yet, as far as we know, in the literature of the color reproduction domain. The Kubelka–Munk formulas can be retrieved from these formulas, with which they have strong connection. The experimental testing shows the good prediction accuracy of the model.

For industrial domains using printed films, in particular the packaging industry, the capacity to predict the color rendering of printed films in superposition with other ones may be helpful for design and color reproduction issues. Even more interesting effects could be obtained by superposing multicolor films so as to show a color image by reflection and a uniform color by transmission [10].

## APPENDIX A: REFLECTANCE AND TRANSMITTANCE OF STACKS OF IDENTICAL FILMS

We have mentioned in Section 5 a stack of  $N$  films having all same angular reflectance  $R$  and transmittance  $T$  for a given incident angle that is not explicit here. We propose to derive the expressions for stacks' front reflectance  $R_N$ , back reflectance  $R'_N$ , front-to-back transmittance  $T_N$ , and back-to-front transmittance  $T'_N$ , respectively given by Eqs. (24), (25), (28), and (29). The demonstration, similar to the one presented in [25] in the context of the Kubelka–Munk model, relies on continuous fractions.

According to Eq. (20), the front reflectances of stacks containing  $N$  and  $N - 1$  films ( $N \geq 2$ ) are related by

$$R_N = R + \frac{TT'}{-R' + \frac{1}{R_{N-1}}}. \quad (\text{A1})$$

Using  $N - 1$  times recursion (A1) until  $R_1 = R$ , one obtains a continued fraction expressing the front reflectance  $R_N$  as a function of  $R$ ,  $R'$ ,  $T$ , and  $T'$ . Every finite continued fraction

$$v_0 + \frac{u_1}{v_1 + \frac{u_2}{v_2 + \dots + \frac{u_k}{v_k}}} \quad (\text{A2})$$

is known to be reducible to a simple fraction, called the  $k$ th convergent of the continued fraction, whose numerator  $U$  and denominator  $V$  are given by the following matrix identity [26]:

$$\begin{pmatrix} \dots & U \\ \dots & V \end{pmatrix} = \begin{pmatrix} 1 & v_0 \\ 0 & 1 \end{pmatrix} \cdot \begin{pmatrix} 0 & u_1 \\ 1 & v_1 \end{pmatrix} \cdot \begin{pmatrix} 0 & u_2 \\ 1 & v_2 \end{pmatrix} \cdots \begin{pmatrix} 0 & u_k \\ 1 & v_k \end{pmatrix}. \quad (\text{A3})$$

The convergent numerator and denominator of the continued fraction expressing  $R_N$  are given by

$$\begin{pmatrix} \dots & U \\ \dots & V \end{pmatrix} = \begin{pmatrix} 1 & R \\ 0 & 1 \end{pmatrix} \cdot \left[ \begin{pmatrix} 0 & TT' \\ 1 & -R' \end{pmatrix} \cdot \begin{pmatrix} 0 & 1 \\ 1 & R \end{pmatrix} \right]^{N-1} \quad (\text{A4})$$

or equivalently by

$$\begin{pmatrix} \dots & U \\ \dots & V \end{pmatrix} = \begin{pmatrix} 0 & 1 \\ 1 & 0 \end{pmatrix} \cdot \begin{pmatrix} 1 & -R' \\ R & TT' - RR' \end{pmatrix}^{N-1} \cdot \begin{pmatrix} 0 & 1 \\ 1 & R \end{pmatrix}. \quad (\text{A5})$$

Let us denote by  $\mathbf{M}$  the matrix raised to the power  $N - 1$  in Eq. (A5). It has two distinct eigenvalues,  $e_1 = 1 - (\alpha + \beta)R$  and  $e_2 = 1 - (\alpha - \beta)R$ , where  $\alpha$  and  $\beta$  are respectively defined by Eqs. (26) and (27). Through matrix diagonalization,  $\mathbf{M}$  may be decomposed as

$$\mathbf{M} = \mathbf{E} \cdot \begin{pmatrix} e_1 & 0 \\ 0 & e_2 \end{pmatrix} \cdot \mathbf{E}^{-1} \quad (\text{A6})$$

with

$$\mathbf{E} = \begin{pmatrix} \alpha - \beta & \alpha + \beta \\ 1 & 1 \end{pmatrix}. \quad (\text{A7})$$

Using a classical result for diagonalizable matrices [27], we have

$$\mathbf{M}^{N-1} = \mathbf{E} \cdot \begin{pmatrix} e_1^{N-1} & 0 \\ 0 & e_2^{N-1} \end{pmatrix} \cdot \mathbf{E}^{-1}. \quad (\text{A8})$$

With this expression for  $\mathbf{M}^{N-1}$ , Eq. (A5) becomes

$$\begin{pmatrix} \dots & U \\ \dots & V \end{pmatrix} = \frac{1}{-2b} \begin{pmatrix} \dots & e_1^N - e_2^N \\ \dots & (\alpha - \beta)e_1^N - (\alpha + \beta)e_2^N \end{pmatrix}. \quad (\text{A9})$$

We deduce the following front reflectance expression:

$$R_N = \frac{e_1^N - e_2^N}{(\alpha - \beta)e_1^N - (\alpha + \beta)e_2^N}, \quad (\text{A10})$$

which becomes, after some rearrangement

$$R_N = \frac{1}{\alpha - \beta \left( 1 - \frac{2}{1 - (e_1/e_2)^N} \right)}. \quad (\text{A11})$$

By a similar reasoning, one gets the back reflectance  $R'_N$  by considering  $R'$  in place of  $R$  and reciprocally. A formula similar to (A11) is obtained, where  $\alpha$ ,  $\beta$ ,  $e_1$ , and  $e_2$  are respectively replaced with

$$\alpha' = \frac{1 - RR' + TT'}{2R'} = \alpha \frac{R}{R'}, \quad (\text{A12})$$

$$\beta' = \sqrt{\alpha'^2 - \frac{R}{R'}} = \beta \frac{R}{R'}, \quad (\text{A13})$$

and

$$e'_{1,2} = 1 - (\alpha' \pm \beta')R' = e_{1,2}. \quad (\text{A14})$$

This finally yields the reflectance formula (28).

Let us now show how to obtain the front-to-back transmittance formula. The transmittance of stacks with  $N$  and  $N - 1$  films are related according to Eq. (23):

$$\frac{T_N}{T_{N-1}} = \frac{T}{1 - R_{N-1}R'}. \quad (\text{A15})$$

$R_{N-1}$  may be replaced with its expanded expression (A10), where  $N$  is replaced with  $N - 1$ . By noting that  $(\alpha - \beta)e_1 = \alpha - \beta - R'$  and  $(\alpha + \beta)e_1 = \alpha + \beta - R'$ , one easily transforms Eq. (A15) into

$$\frac{T_N}{T_{N-1}} = T \frac{u_{N-1}}{u_N}, \quad (\text{A16})$$

where  $u_k$  is defined for every integer  $k$  as

$$u_k = (\alpha - \beta)e_1^k - (\alpha + \beta)e_2^k. \quad (\text{A17})$$

Noting that  $u_1 = -2b$ , we may thus write  $T_N$  as the following product where the brackets contain  $N - 1$  fractions whose numerators and denominators mutually cancel except  $u_1$  and  $u_N$ :

$$T_N = T \left( \frac{T_N}{T_{N-1}} \cdot \frac{T_{N-1}}{T_{N-2}} \cdots \frac{T_2}{T} \right) = T^N \left( \frac{u_{N-1}}{u_N} \cdot \frac{u_{N-2}}{u_{N-1}} \cdots \frac{u_1}{u_2} \right) = T^N \left( \frac{-2b}{u_N} \right), \quad (\text{A18})$$

which finally yields

$$T_N = \frac{2bT^N}{(\alpha + \beta)e_2^N - (\alpha - \beta)e_1^N}. \quad (\text{A19})$$

The back-to-front transmittance formula is obtained in the same way by replacing  $T$  with  $T'$ , which yields  $T'^N$  in place of  $T^N$  at the numerator of the fraction in Eq. (A19).

## ACKNOWLEDGMENTS

The authors would like to express their gratitude to Mr. Hugo Cayla from Institut d'Optique Graduate School (IOGS) for his contribution to the experiments, as well as Jean-Marie Becker and Pierre Chavel from the ERIS group in the Hubert Curien Laboratory for interesting discussions related to this study.

## REFERENCES

1. P. Kubelka, "New contributions to the optics of intensely light-scattering material. Part I," *J. Opt. Soc. Am.* **38**, 448–457 (1948).
2. S. Mourad, P. Emmel, K. Simon, and R. D. Hersch, "Extending Kubelka-Munk's theory with lateral light scattering," in *Proceedings of IS&T NIP17: International Conference on Digital Printing Technologies*, Fort Lauderdale, Fla., USA (2001), pp. 469–473.
3. L. Yang and B. Kruse, "Revised Kubelka–Munk theory. I. Theory and application," *J. Opt. Soc. Am. A* **21**, 1933–1941 (2004).
4. L. Yang, B. Kruse, and S. J. Miklavcic, "Revised Kubelka–Munk theory. II. Unified framework for homogeneous and inhomogeneous optical media," *J. Opt. Soc. Am. A* **21**, 1942–1952 (2004).
5. L. Yang and S. J. Miklavcic, "Revised Kubelka–Munk theory. III. A general theory of light propagation in scattering and absorptive media," *J. Opt. Soc. Am. A* **22**, 1866–1873 (2005).
6. F. Rousselle, M. Hébert, and R. D. Hersch, "Predicting the reflectance of paper dyed with ink mixtures by describing light scattering as a function of ink absorbance," *J. Imaging Sci. Technol.* **54**, 050501 (2010).
7. M. Hébert, R. D. Hersch, and L. Simonot, "Spectral prediction model for piles of nonscattering sheets," *J. Opt. Soc. Am. A* **25**, 2066–2077 (2008).
8. P. Emmel, I. Amidror, V. Ostromoukhov, and R. D. Hersch, "Predicting the spectral behavior of colour printers for transparent inks on transparent support," in *Proceedings of IS&T/SID 96 Color Imaging Conference* (Society for Imaging Science, 1996), pp. 86–91.
9. F. R. Ruckdeschel and O. G. Hauser, "Yule-Nielsen effect in printing: a physical analysis," *Appl. Opt.* **17**, 3376–3383 (1978).
10. J. Machizaud and M. Hébert, "Spectral transmittance model for stacks of transparencies printed with halftone colors," in *SPIE/IS&T Color Imaging XVII: Displaying, Processing, Hardcopy, and Applications* (Society for Imaging Science and Technology, 2012).
11. M. Born, E. Wolf, and A. Bhatia, *Principles of Optics: Electromagnetic Theory of Propagation, Interference and Diffraction of Light* (Cambridge University, 1999).
12. M. E. Demichel, *Procédés* **26**, 17–21 (1924).
13. J. A. S. Viggiano, "The color of halftone tints," *Proc. TAGA* **37**, 647–661 (1985).
14. J. A. C. Yule and W. J. Nielsen, "The penetration of light into paper and its effect on halftone reproduction," *Proc. TAGA* **3**, 65–76 (1951).
15. M. Hébert and R. D. Hersch, "Yule–Nielsen based recto–verso color halftone transmittance prediction model," *Appl. Opt.* **50**, 519–525 (2011).
16. R. D. Hersch and F. Crété, "Improving the Yule-Nielsen modified spectral Neugebauer model by dot surface coverages depending on the ink superposition conditions," *Proc. SPIE* **5667**, 434–445 (2005).
17. J. Machizaud and M. Hébert, "Spectral reflectance and transmittance prediction model for stacked transparency and paper both printed with halftone colors," *J. Opt. Soc. Am. A*, **29**, 1537–1548 (2012).
18. G. Sharma, *Digital Color Imaging Handbook* (CRC, 2003).
19. P. Kubelka, "New contributions to the optics of intensely light-scattering materials, part II: Non homogeneous layers," *J. Opt. Soc. Am.* **44**, 330–335 (1954).
20. V. Ostromoukhov and R. D. Hersch, "Stochastic clustered-dot dithering," *J. Electron. Imaging* **8**, 439–445 (1999).
21. B. Maheu, J. N. Letouzan, and G. Gouesbet, "Four-flux models to solve the scattering transfer equation in terms of Lorentz-Mie parameters," *Appl. Opt.* **23**, 3353–3362 (1984).
22. P. S. Mudgett and L. W. Richards, "Multiple scattering calculations for technology," *Appl. Opt.* **10**, 1485–1502 (1971).
23. S. Chandrasekhar, *Radiative Transfer* (Dover, 1960).
24. K. Klier, "Absorption and scattering in plane parallel turbid media," *J. Opt. Soc. Am.* **62**, 882–885 (1971).
25. M. Hébert and J.-M. Becker, "Correspondence between continuous and discrete two-flux models for reflectance and transmittance of diffusing layers," *J. Opt. A* **10**, 035006 (2008).
26. C. K. Yap, *Fundamental Problems of Algorithmic Algebra* (Oxford University, 2000).
27. G. Strang, *Applied Mathematics* (MIT, 1986).